

1 **An analytical approach to determine the optimal length of paired drip** 2 **laterals in uniformly sloped fields**

3
4 Giorgio Baiamonte¹, Giuseppe Provenzano², Giovanni Rallo³

5
6 ¹Associate Professor. Dipartimento di Scienze Agrarie e Forestali (SAF), Università di
7 Palermo, Viale delle Scienze 12, 90128 Palermo, Italy. Corresponding Author:
8 giorgio.baiamonte@unipa.it

9 ²PhD, Associate Professor. Dipartimento di Scienze Agrarie e Forestali (SAF), Università di
10 Palermo, Viale delle Scienze 12, 90128 Palermo, Italy.

11 ³PhD, Fellowship Researcher. Dipartimento di Scienze Agrarie e Forestali (SAF), Università
12 di Palermo, Viale delle Scienze 12, 90128 Palermo, Italy.

13 14 **Abstract**

15
16 Microirrigation plants, if properly designed, allow to optimize water use efficiency and to
17 obtain quite high values of emission uniformity in the field. Disposing paired laterals, for
18 which two distribution pipes extend in opposite directions from a common manifold, can
19 contribute to reduce the initial investment cost, that represents a limiting factor for small-scale
20 farmers of developing countries where, in the last decade, the diffusion of such irrigation
21 system has been increasing.

22 Objective of the paper is to propose an analytical approach to evaluate the maximum lengths
23 of paired drip laterals for any uniform ground slope, respecting the criteria to maintain emitter
24 flow rates or the corresponding pressure heads within fixed ranges in order to achieve a
25 relatively high field emission uniformity coefficient.

26 The method is developed by considering the motion equations along uphill and downhill sides
27 of the lateral and the hypothesis to neglect the variations of emitters' flow rate along the
28 lateral as well as the local losses due to emitters' insertions.

29 If for the uphill pipe, the minimum and the maximum pressure heads occurs at the upstream
30 end and at the manifold connection respectively, on the downhill side, the minimum pressure
31 head is located in a certain section of the lateral, depending on the geometric and hydraulic
32 characteristics of the lateral, as well as on the slope of the field; a second relative maximum
33 pressure head could also exist at the downstream end of the pipe.

34 The proposed methodology allows in particular to determine separately the number of
35 emitters in uphill and downhill sides of the lateral and therefore, once fixing emitter's
36 spacing, the length of the uphill and downhill laterals and the position of the manifold.

37 Applications and validation of the proposed approach, considering different design
38 parameters, are finally presented and discussed.

39

40 **Key-words**

41 Microirrigation, Paired laterals, Optimal length

42

43 **Introduction**

44

45 Microirrigation is considered a convenient and efficient system allowing to keep the crop
46 water demand to a minimum, while maintaining current levels of crop production; for this
47 reason it is mostly used in arid regions where water resources for irrigation are limited.

48 The adoption and diffusion of microirrigation technology, in developed and developing
49 countries, is consequent to economic factors (water price, cost of equipment, crop price), farm
50 organization (size of the farm, experience of the farmer) and environmental conditions
51 (precipitation, soil quality) (Genius et al, 2012).

52 Mainly in developing countries, small-scale farmers, have been sometimes reluctant to adopt
53 this system due to the initial investment cost required for the equipment, that may be higher
54 than those of other irrigation options.

55 In order to optimize water use efficiency and to reduce the initial investment cost, the design
56 of the submain unit and its proper management play a key role to maximizing the emitter
57 uniformity and the profitability of the investment. When using non pressure compensating
58 emitters, the first step for designing a submain considers a range of pressure variation along
59 the lateral, which can contribute to obtain the desired uniformity of water distribution in the
60 entire submain. In fact, limiting the range of pressure head makes it possible to reduce the
61 variability of flow rates discharged by the installed emitters.

62 The criterion of limiting the variation of emitter discharge to about $\pm 5\%$ of the nominal flow
63 rate or, alternatively, the variation of pressure head to about $\pm 10\%$ of its nominal value, in
64 order to obtain reasonable high values of distribution uniformity coefficients has been widely
65 used to design drip irrigation single laterals or entire submains. Provenzano (2005)
66 demonstrated that when the exponent x of the flow rate-pressure head relationship is equal to
67 0.5 and emitters are characterized by a good quality (emitters' manufacturer's variation

68 coefficient $CV \leq 0.03$), such variation of discharge corresponds to a pressure variations of
69 about 20% of the nominal value, and determines values of emission uniformity coefficient
70 EU, as defined by Karmeli and Keller (1975), equal to $EU = 90\%$ or higher. Of course, the
71 higher the emitter' CV value, the larger the interval of variability of the flow rates around the
72 average value whereas, for a fixed CV, a lower variability of emitter flow rates is always
73 related to a higher distribution uniformity.

74 Moreover, using paired laterals for which two distribution pipes extend in opposite directions
75 from a common manifold, as represented in fig. 1, for a fixed pipe diameter, can allow
76 maximizing the lateral length while maintaining the pressure variations within the considered
77 range, so that the initial investment cost of the system can be reduced. Al-Samarmad (2002),
78 considering two design criteria to determine lateral and manifold lengths for a given subunit
79 and using local prices for installing and operating micro irrigation systems, found that the
80 subunit cost decreases as lateral length increases up to a certain limit and then it starts to
81 increase again.

82 The importance of an adequate analysis of trickle lateral hydraulics aimed to find the optimal
83 length or diameter of laterals laid on sloping fields has been emphasized by Kang et al.,
84 (1996). In particular, the forward Step by Step (SBS) procedure, as unanimously recognized,
85 represents the most affordable method to evaluate pressure heads and actual flow rates
86 corresponding to all the emitters in the lateral even if, when applied from the uphill end to the
87 downhill end of the lateral, allows to find the solution after tedious and time consuming
88 iterations.

89 Despite a detailed analysis should require the evaluation of local losses due to emitter's
90 insertion, whose importance has been emphasized by several Authors (Al Amoud, 1995,
91 Bagarello et al., 1997, Juana et al., 1992, Provenzano et al., 2007), in all the cases when the
92 number of emitter in the lateral and/or the variations of flow velocity due to the emitter
93 connections are limited, such losses can be neglected. In fact, considering that local losses are
94 usually evaluated as an α fraction of flow kinetic head, Provenzano and Pumo (2004) verified
95 that local losses result less than 10% of the total losses for in-line emitters characterized by
96 $\alpha \leq 0.3$ and spaced 1.0 m or more. More recently, Provenzano et al. (2014) on the basis of
97 experiments carried out on five different commercial lay-flat drip tapes, due to the generally
98 low values of α characterizing the emitters, evidenced that neglecting local losses generates
99 an overestimation of the lateral lengths with differences equal to 8.9%, 3.6% and 1.6%, when
100 emitter spacing is equal to 20 cm, 50 cm and 100 cm respectively.

101 When designing paired laterals, it is fundamental to evaluate the best position of the submain
102 pipe (BSP), which was defined by Keller and Bliesner (2001) as the location of the manifold
103 determining the same minimum pressure in uphill and downhill laterals. On level ground the
104 length of both laterals is identical, whereas for any other field slope, the manifold has to be
105 shifted uphill, in a position that balances the differences in elevation and pressure losses in
106 both sides of the laterals. Based on their definition, Keller and Bliesner (2001) developed
107 graphical and numerical solution methods.

108 In order to obtain the required uniformity of water application, Kang and Nishiyama (1996)
109 proposed a method for design single and paired laterals laid on both flat and sloped fields
110 based on the finite element method and the golden section search (Gill et al., 1989). For
111 paired laterals, the method allows to obtain the operating pressure head and the BSP at which
112 the maximum uniformity is produced for a fixed emitter discharge, once the lateral length or
113 pipe diameter and other field conditions are given.

114 Recently, Jiang and Kang (2010), using the energy gradient line approach (Wu, 1975; Wu and
115 Gitlin, 1975, Wu et al., 1986), proposed the best equation form aimed to evaluate the BSP
116 according to the definition provided by Keller and Bliesner (2001) and developed a simple
117 procedure to design paired laterals on sloped fields.

118 In this study, an analytical approach to design the optimal length of paired drip laterals laid on
119 uniformly sloped fields and to determine the position of the manifold, under the hypotheses to
120 neglect local losses due to the emitters' connections, is presented and discussed. Application
121 and validation of the proposed approach, covering a combination of different design
122 parameters, is finally presented and discussed.

123

124 **Theory**

125

126 Fig. 1 illustrates the typical layout of a submain in which the manifold, placed in a generic
127 position, divides each lateral into two sections - uphill and downhill - of different length
128 (paired lateral). Fig. 2 shows the scheme of a single paired lateral characterized by a length L
129 and multiple outlets spaced S , laid on an uniformly sloped field. In the figure, the connection
130 between the manifold and the lateral, the hydraulic grade line and the pressure head
131 distribution are schematically illustrated. As can be observed, n_u and n_d indicate the number of
132 emitters along the uphill and the downhill sides of the lateral, with n the total number of
133 emitters, whereas i_{min} , represents the number of emitters installed in the downhill side of the
134 lateral, from the manifold connection to the pipe section with the minimum pressure head.

135 For the uphill pipe, the minimum pressure head, $h_{\min}^{(u)}$, arises at the upstream end, whereas the
 136 maximum pressure head, $h_{\max}^{(u)}$, is at the manifold connection. On the other side, according to
 137 the geometric and hydraulic characteristics of the lateral, as well as to the slope of the field,
 138 the minimum pressure head for the downhill pipe, $h_{\min}^{(d)}$, can be located in a certain section of
 139 the lateral, whereas a second relative maximum pressure head, $h_{\max}^{(d)}$, could also exist at the
 140 downstream end of the pipe.

141 In order to achieve a relatively high field emission uniformity coefficient along the lateral, it
 142 is necessary to limit the variations of pressure head due to elevation changes and head losses.
 143 Therefore, indicating h_n the nominal pressure head of the emitter, the hydraulic design criteria
 144 of the lateral here considered, assumes that the working pressure heads of the generic emitter,
 145 h_i , in both uphill and downhill sides, have to be in the range between $0.9 h_n$ and $1.1 h_n$.

146 For a lateral with given geometric and hydraulic characteristics, laid on an uniformly sloped
 147 field, according to the fixed maximum variations of pressure heads and to the elevation
 148 changes, an optimal (maximum) length, L_{opt} , can be identified.

149 In small diameter polyethylene pipes (PE), friction losses per unit pipe length, J , can be
 150 evaluated with the Darcy-Weisbach equation:

$$151 \quad J = \frac{f V^2}{D 2g} \quad (1)$$

152 where f [-] is the friction factor, V is the mean flow velocity [m/s], D [m] is the internal pipe
 153 diameter and g [m²/s] is the acceleration of gravity. According to the Blasius equation,
 154 friction factor can be expressed, as a function of Reynolds number R :

$$155 \quad f = 0.316 R^{-0.25} \quad (2)$$

156 For a single lateral ($n_u = 0$) with n emitters, under the hypothesis to neglect the variation of
 157 flow rates discharged by the emitters, the total friction losses between the first and the last
 158 emitter of the lateral, $\Delta h_f^{(d)}$, can be easily calculated according to Provenzano et al., (2005):

$$159 \quad \Delta h_f^{(d)} = 0.0235 \frac{V^{0.25} S q_n^{1.75}}{D^{4.75}} \sum_{i=1}^{n-1} i^{1.75} \quad (3)$$

165 where ν [$\text{m}^2 \text{s}^{-1}$] is the water kinematic viscosity, S [m] is the emitter spacing, q_n [$\text{m}^3 \text{s}^{-1}$] is the
 166 average emitter discharge corresponding to h_n and i [-] is the generic emitter installed along
 167 the lateral.

168 In order to find analytical solution to design sloping laterals, the generalised harmonic number
 169 can be introduced into eq. (3):

170

$$171 \quad \Delta h_f^{(d)} = K S H_{n-1}^{(-1.75)} \quad (4)$$

172

173 where $H(.,.)$ is the generalised harmonic number in power -1.75, truncated at n , and K (-) is a
 174 parameter that, for the selected resistance law, depends on pipe diameter and emitter flow
 175 rate, as following:

176

$$177 \quad K = 0.0246 \frac{V^{0.25} q_n^{1.75}}{D^{4.75}} \quad (5)$$

178

179 For a given lateral K is constant and assumes value ranging in the interval between 1.00e-05
 180 and 1.00e-03, as evaluated according to the common ranges of variability of q_n ($4 \text{ l/h} < q_n <$
 181 25 l/h) and D ($0.012 \text{ m} < D < 0.020 \text{ m}$).

182 Accounting for the differences in emitters elevation and neglecting the kinetic head, the
 183 motion equation allows to determine the pressure head of the i -th emitter, h_i , along the uphill
 184 side, $h_i^{(u)}$, as well as along the downhill side of the lateral, $h_i^{(d)}$, as:

185

$$186 \quad h_i^{(u)} = h_{\max}^{(u)} - \Delta h_f^{(u)} + K S H_{n_u-i}^{(-1.75)} + i S S_0 \quad (6a)$$

$$187 \quad h_i^{(d)} = h_{\max}^{(d)} - \Delta h_f^{(d)} + K S H_{n_d-i}^{(-1.75)} - i S S_0 \quad (6b)$$

188

189 in which S_0 [-] is the field slope (negative downhill). Moreover, according to eq. (4), the total
 190 head losses in the uphill, $\Delta h_f^{(u)}$, and in the downhill, $\Delta h_f^{(d)}$, laterals can be evaluated as:

191

$$192 \quad \Delta h_f^{(u)} = K S H_{n_u}^{(-1.75)} \quad (7a)$$

$$193 \quad \Delta h_f^{(d)} = K S H_{n_d}^{(-1.75)} \quad (7b)$$

194

195 If considering the uphill side of the lateral, by imposing equal to 0.9 h_n the minimum allowed
 196 pressure head, $h_{\min}^{(u)}$, at the end of the lateral, and equal to 1.1 h_n the maximum pressure head at
 197 the manifold connection, eq. 6a, for $i = n_u$, can be rewritten as:

198

$$199 \quad 0.9h_n = 1.1h_n - \Delta h_f^{(u)} + n_u S S_0 \quad (8)$$

200

201 By introducing eq. (7a) into eq. (8) and by normalising the pressure head respect to S , the
 202 number of emitters in the uphill lateral, n_u , corresponding to the optimal (maximum) value,
 203 can be implicitly expressed as:

204

$$205 \quad n_u = \frac{K}{S_0} H_{n_u, opt}^{(-1.75)} - 0.2 \frac{h_n}{S_0 S} \quad (9)$$

206

207 Contrarily to eq. (6a) in which $h_i^{(u)}$ monotonically decreases with increasing i , and therefore
 208 the lowest pressure head occurs at the uphill end of the lateral, eq. (6b) admits a minimum
 209 value of pressure head, $h_{\min}^{(d)}$, in a certain section of the downhill lateral. In order to know the
 210 exact location of this minimum, it is necessary to derive eq. (6b) with respect to i . The
 211 derivative of a discrete variable, as i was denoted, exists for any i value under the assumption
 212 that $di = dS/S$. Thus, the partial derivative of eq. (6b) respect to i , yields:

213

$$214 \quad \frac{\partial h_i^{(d)}}{\partial i} = -S S_0 + 1.75K S \left(\zeta(-0.75) - H_{n_d-i}^{(-0.75)} \right) \quad (10)$$

215

216 in which $H_{n_d-i}^{(-0.75)}$ is the generalised harmonic number and $\zeta(.,.)$ is the Riemann Zeta function
 217 of argument $(.)$, equal respectively to:

218

$$219 \quad H_{n_d-i}^{(-0.75)} = \sum_{i=1}^{n_d-i} i^{0.75} \quad (11)$$

220

$$221 \quad \zeta(-0.75) = -\frac{1}{1.75} + \sum_{n=0}^{\infty} (-1)^n \frac{\gamma_n (-1.75)^n}{n!} = -0.1336 \quad (12)$$

222

223 where γ_n are the Stieltjes constants. The Riemann Zeta function of eq. (12) is a particular case
 224 of the more general Hurwitz–Lerch Zeta function (Agnese et al., 2014). By imposing eq. (10)
 225 equals to zero, the emitter, i_{min} , in which the minimum pressure head, $h_{min}^{(d)}$ is located, can be
 226 determined by solving the following implicit equation:

$$228 \quad H_{n_d - i_{min}}^{(-0.75)} = \zeta(-0.75) - \frac{S_0}{1.75K} \quad (13)$$

229
 230 As expected, eq. (13) shows that i_{min} only depends on the number of the emitters along the
 231 downhill side of the lateral, n_d , on the value of K , as well as on the slope of the lateral, S_0 , but
 232 it is interesting to notice that it does not depend on the spacing S .

233 Fig. 3 shows, for different K values, the distance $n_d - i_{min}$, between the point (emitter)
 234 characterized by the minimum pressure head ($h_i = h_{min}^{(d)}$) and the downhill end of the lateral,
 235 as a function of the lateral slope. As can be observed, the value $n_d - i_{min}$ increases with
 236 increasing S_0 , whereas for a fixed S_0 , the position $n_d - i_{min}$ increases with decreasing K .

237 In the particular case of a lateral laid on a level field ($S_0 = 0$), as evident, the minimum
 238 pressure head is located at the downstream end of the lateral ($i_{min} = n_d$), for any K value. On
 239 the other hand, for a fixed K , the position of the emitter with the minimum pressure in the
 240 downhill lateral head, at rising S_0 , shifts uphill.

241 In order to determine the maximum number of emitters in the downhill lateral, it could be
 242 possible i) to fix the minimum allowed pressure head at $i = i_{min}$ and to control that $h_{max}^{(d)} \leq 1.1$
 243 h_n or alternatively ii) to fix the maximum allowed pressure head at the end of the downhill
 244 lateral and verifying that $h_{min}^{(d)} \geq 0.9 h_n$. However, according to the results of application (not
 245 showed), the former option provides a maximum number of emitters always higher than the
 246 latter. Thus, in order to determine the maximum number of emitters in the downhill lateral,
 247 the relative minimum admissible pressure head ($0.9 h_n$) at $i = i_{min}$, has be imposed into eq.
 248 (6b):

$$250 \quad -0.2 \frac{h_n}{S} = -K H_{n_d}^{(-1.75)} + K H_{n_d - i_{min}}^{(-1.75)} - i_{min} S_0 \quad (14)$$

251
 252 To find the value n_d satisfying the imposed condition for any fixed slope of the lateral, the
 253 system of eqs. (13) and (14) has to be solved. However, the solution in terms of the pairs (n_d ,
 254 i_{min}) could determine, for $i > i_{min}$, pressure heads higher than $1.1 h_n$. This last condition occurs

255 for ground slope higher than a threshold value, $|S_0^{th}|$, representing the maximum value for
 256 which operating pressure heads along the entire downhill lateral are in the desired range.

257 In order to find $|S_0^{th}|$ and the associated optimal number of emitters in the downhill lateral,
 258 $n_{d,opt}^{th}$, the maximum pressure head at the end of the lateral has also to be fixed to the
 259 maximum admitted value (i.e. for $i = n_d$, $h_{max}^{(d)} = 1.1 h_n$). Thus, by using eq. (7b) and by
 260 considering that for $i = n_d$, $H_{n_d-i}^{(-1.75)} = 0$, eq. (6b) can be rearranged as:

261

$$262 \quad n_{d,opt}^{th} S_0^{th} + K H_{n_{d,opt}^{th}}^{(-1.75)} = 0 \quad (15)$$

263

264 The system represented by eqs. (13), (14) and (15) can be solved in terms of $n_{d,opt}^{th}$, i_{min} and
 265 $|S_0^{th}|$, so that, once $n_{d,opt}^{th}$ is known, the optimal length of the entire lateral, corresponding to
 266 the threshold ground slope, can be determined as $n_{opt}^{th} = n_{u,opt}^{th} + n_{d,opt}^{th}$.

267

268 **Examples of application**

269

270 In the following examples the proposed procedure is applied in order to determine the
 271 maximum number of emitters in a paired lateral, under different internal pipe diameters, D ,
 272 nominal pressure heads, h_n , emitter spacing, S , and flow rates, q_n , for two different ground
 273 slopes, S_0 .

274 The first case is related to a lateral with $D = 20$ mm, $q_n = 20$ l/h and considers two values of
 275 the ratio h_n/S ($h_n/S = 20$ and $h_n/S = 40$). According to eq. (5), K value is equal to $5.82e-05$.

276 In Fig. 4a-b the number of emitters in the uphill lateral, n_u , evaluated with eq. 9, the pairs n_d ,
 277 i_{min} , obtained by solving eqs. (13) and (14), as well as the sum, $n_d + n_u$, are represented as a
 278 function of the lateral slope $|S_0|$, for $h_n/S = 20$ (Fig. 4a) and for $h_n/S = 40$ (Fig. 4b). In the
 279 secondary vertical axes, the dimensionless nominal pressure head at the end of the downhill
 280 lateral, $h_{max}^{(d)} / S$, as well as the minimum and the maximum, $0.9 h_n/S$ and $1.1 h_n/S$, are also
 281 showed. As expected, with increasing $|S_0|$, n_u decreases whereas n_d increases, being the values
 282 n_u and n_d equals for $S_0 = 0$, and therefore when the manifold connection is placed in the
 283 middle of the lateral. As an example, for $h_n/S = 20$ (Fig. 4a), the optimal number of emitters
 284 along the entire lateral, $n_{opt} = n_u + n_d$, results maximum ($n_{opt} = 165$) for $S_0 = 0$ and decreases
 285 with increasing $|S_0|$, until reaching a minimum value, $n_{opt}^{th} = 158$, for $|S_0| = |S_0^{th}|$, being $|S_0^{th}| =$

286 9.4 %. As can be observed in Fig. 4a, even if for any $|S_0| > |S_0^{th}|$, an optimal number of
 287 emitters n_{opt} higher than n_{opt}^{th} could be evaluated, the solution cannot be accepted because the
 288 pressure head at the downhill end of the lateral results higher than the maximum allowable. In
 289 fig. 4a, it can also be noticed that, at increasing $|S_0|$, the location of the minimum pressure head
 290 (dashed curve) shifts upstream, as a consequence of the results illustrated in fig. 3, passing
 291 from $i_{min} = 83$ (downhill end of the lateral) for $S_0 = 0$ to $i_{min} = 53$ for $S_0 = S_0^{th} = -9,4\%$.
 292 Similar observations can be evidenced in the case of $h_n/S = 40$ (Fig. 4b), to which correspond
 293 an optimal number of emitters $n_{opt} = 212$ for $S_0 = 0$ and $n_{opt}^{th} = 204$ ($n_{u,opt}^{th} = 48$, $n_{d,opt}^{th} = 156$)
 294 evaluated for the threshold slope $S_0^{th} = -14,6\%$.

295 Moreover, the value of the normalized pressure head at the end of the lateral, $h_{max}^{(d)} / S$,
 296 increases with the slope, becoming higher than $1.1 h_n/S$ for $|S_0| > |S_0^{th}|$, as can be analytically
 297 quantified by solving the system of eqs. (13), (14) and (15). Of course, all the solutions
 298 obtained for $|S_0| > |S_0^{th}|$ cannot be accepted.

299 The second examined case corresponds to a lateral having internal diameter $D = 16$ mm and
 300 nominal emitters discharge, associated to the pressure head h_n , $q_n = 4$ l/h ($K = 1.00e-05$).

301 Similarly to Fig. 4a-b, Fig. 5a-b shows the number of emitters in the uphill, n_u , and downhill
 302 n_d , lateral, the values i_{min} , as well as the sum, $n_d + n_u$, as a function of the lateral slope $|S_0|$,
 303 and allows one to evaluate the optimal lateral length for $h_n/S = 20$ (Fig. 5a) and for $h_n/S = 40$
 304 (Fig. 5b).

305 As an example, for $h_n/S = 20$ and a field slope equal to -2.0% , the number of emitters in the
 306 uphill and in the downhill sides of the lateral result of 115 and 190 ($n_{opt} = 305$), respectively,
 307 to which corresponds acceptable values of the ratio $h_{max}^{(d)} / S$ that, at the end of the lateral, is
 308 equal to 19.0, whereas for $S_0 = S_0^{th} = -5.0\%$, $n_{opt}^{th} = 300$ is obtained by summing $n_{u,opt}^{th} = 71$
 309 and $n_{d,opt}^{th} = 229$.

310 If comparing the results of the two considered examples, it can be observed that to the lower
 311 K value (second example) corresponds, for any field slope, an optimal number of emitters
 312 systematically higher than that obtained in the first example. In particular, for $K = 5.82e-05$
 313 and a field slope of -2% , the optimal number of emitters results equal to 163.

314 By the analysis of Fig. 4 and Fig. 5, it is possible to verify that n_{opt}^{th} corresponds to the
 315 maximum number of the emitters in a lateral laid on a ground having slope equal to $|S_0^{th}|$, for
 316 which operating pressure heads are in the admissible range ($0.9 h_n/S \div 1.1 h_n/S$); in particular,

317 for $n = n_{opt}^{th}$, the minimum pressure head, $0.9 h_n/S$, is imposed at $h_{min}^{(u)}$ and $h_{min}^{(d)}$, whereas the
318 maximum, $1.1 h_n/S$, is imposed at $h_{max}^{(u)}$ and $h_{max}^{(d)}$ (Fig. 2). Thus, the knowledge of n_{opt}^{th} and
319 $|S_0^{th}|$ has interesting implications when the optimal length of paired laterals in uniformly
320 sloped ground has to be evaluated. In fact, for a lateral of fixed geometric and hydraulic
321 characteristics, any field slope lower than $|S_0^{th}|$ determines acceptable solutions in terms of
322 maximum number of emitters to be installed along the entire lateral, with pressure heads
323 always within the admitted range. The contemporary knowledge of the corresponding number
324 of emitters in the uphill lateral, allows one to establish the position of the manifold
325 connection. On the other hand, if field slope $|S_0|$ is higher than $|S_0^{th}|$, the corresponding n_d
326 determines unacceptable pressure heads at the end of the lateral, higher than the maximum
327 allowed.

328 To generalize the results to the usual values of discharges and internal diameters, i.e. $K =$
329 $1.00e-05 \div 1.00e-03$, the system of eqs. (13), (14) and (15) has been solved in terms of
330 $n_{d,opt}^{th}, i_{min}$ and S_0^{th} , in order to obtain, as a function of K , the optimal length of the entire
331 lateral, $n_{opt}^{th} = n_{u,opt}^{th} + n_{d,opt}^{th}$, corresponding to the particular case for which $|S_0| = |S_0^{th}|$.

332 Fig. 6 shows, as a function of K , the number of the emitters in uphill, n_u^{th} and downhill n_d^{th}
333 laterals, the location of the emitter with the minimum pressure head, i_{min} , as well as the
334 optimal number of emitters in the entire lateral $n_{opt}^{th} = n_u^{th} + n_d^{th}$, for $h_n/S = 20$ (Fig. 6a) and for
335 $h_n/S = 40$ (Fig. 6b). In the secondary vertical axes, the threshold value of the slope, $|S_0^{th}|$, is
336 also represented as a function of K . The black dots indicate the threshold values of $|S_0^{th}|$, for
337 both $K = 5.82e-05$ and $K = 1.00e-05$, for $h_n/S = 20$ (Fig. 6a) and $h_n/S = 40$ (Fig. 6b).

338 Analysis of Fig. 6a,b evidences, as expected, that parameter K determines a noticeable
339 influence on the number of emitters (optimal lateral length). In particular, for both the
340 selected values of h_n/S (20 and 40), the higher the value of K (higher q_n or lower D) the lower
341 the number of emitters. Moreover, for a fixed K , the threshold ground slope increases with
342 h_n/S . As an example, for $K = 1.00e-4$, $|S_0^{th}|$ is equal to -11.4 % and -17.7 %, for $h_n/S = 20$ and
343 $h_n/S = 40$, respectively. Finally, for any K value, increasing h_n/S from 20 to 40, determines a
344 constant increment, equal to 29%, of the optimal number of emitters to be installed and
345 therefore of the optimal length of the lateral.

346

347

348 **Validation of the proposed approach**

349

350 The validity of the proposed approach has been assessed on terms of its ability to predict the
351 variations of pressure heads along the lateral and consequently, for a certain model of emitter,
352 to estimate the distribution of discharged flow rates, according to the actual flow rate-pressure
353 head relationship. In particular, using the iterative forward step-by-step (SBS) procedure,
354 starting from the manifold connection to the end of both the downhill and the uphill sides of
355 the lateral, it was possible to evaluate the differences on operating pressure heads and the
356 subsequent errors in emitter flow rates, associated to the hypothesis of a constant emitter
357 discharge ($x = 0$) assumed to derive eq. (3).

358 Towards this aim, the SBS procedure has been applied for a lateral characterized by $D = 20$
359 mm and $q_n = 20$ l/h ($K = 5.82e-05$) laid i) on a field slope $S_0 = S_0^{th} = -9.4\%$, as obtained for
360 $h_n/S = 20$ (case A, $n_u^{th} = 38$, $n_d^{th} = 120$) and ii) on a field slope $S_0 = S_0^{th} = -14.6\%$ as evaluated
361 for $h_n/S = 40$ (case B, $n_u^{th} = 48$, $n_d^{th} = 156$). In the former case an emitter spacing $S = 1.0$ m was
362 considered, whereas in the latter $S = 0.5$ m, so that in both cases h_n resulted equal to 20 m.
363 Moreover, two different flow rate-pressure head relationships ($q = k h^x$) expressed by $k =$
364 $1.24e-06$ m²/s and $x = 0.5$ (case A1 and B1), and by $k = 2.87e-07$ m²/s and $x = 1.0$ (case A2 and
365 B2), were examined.

366 Fig. 7a,b shows the distributions of pressure heads along the lateral evaluated for case A and
367 B respectively, under the hypothesis of constant emitter flow rates ($x = 0$) or assuming the
368 other two flow rate-pressure head relationships obtained for $x = 0.5$ and $x = 1.0$. According to
369 the results, on both the uphill and downhill sides of the lateral, the value of pressure head
370 corresponding to the generic emitter tends to rise at increasing x , with maximum differences,
371 for $x = 0.5$ and for $x = 1.0$, equal respectively to -1.12 % and -1.74 % for case A, and to -1.47
372 % and -2.24 % for case B. Therefore, the assumption of a constant emitter flow rate
373 determines a quite slight underestimation of the operating emitter pressure heads along the
374 entire lateral. It is also interesting to observe that the position where the minimum pressure
375 head occurs does not depend on the value of the exponent of the flow rate-pressure head
376 relationship. Fig. 8a,b shows, for case A and case B, as a function of the lateral length, the
377 errors on flow rates calculated by considering the pressure head distribution obtained with the
378 proposed approach ($x = 0$) and the corresponding actual values determined by using the SBS
379 procedure for $x = 0.5$ and $x = 1.0$, expressed as a percentage of the latter. As can be observed,
380 for case A, the errors associated to the discharged flow rates result lower than -0.56 % and -

381 1.74 % for $x = 0.5$ and $x = 1.0$, whereas, for case B, lower than -0.74 % and -2.24 % for $x =$
382 0.5 and $x = 1.0$, and therefore always insignificant for practical applications.

383

384 **Conclusions**

385

386 The paper presents an analytical approach to evaluate the optimal length of paired drip laterals
387 placed on uniformly sloped grounds. In particular, once fixed the geometric and hydraulic
388 characteristics of the lateral, the maximum number of emitters in the uphill and downhill sides
389 and therefore the optimal lateral length and the position of the manifold, can be determined by
390 considering a simplified friction losses evaluation procedure, that assumes constant emitter
391 flow rates and the criteria to fix the variation of pressure head to $\pm 10\%$ of its nominal value
392 along the entire lateral. The methodology neglects local losses, so that it can be applied when
393 the morphology of emitter connections do not produce significant reductions of the lateral
394 cross section.

395 Two examples of application of the proposed approach, covering different values of nominal
396 flow rates and internal pipe diameters (summarized in a single variable, K) and for different
397 combinations of the nominal pressure head and emitter spacing (h_n/S), are presented and
398 discussed. Application of the procedure evidenced that, for any field slope, the optimal
399 number of emitters in the paired lateral increases at decreasing K . Moreover, by fixing K and
400 h_n/S , it exists a threshold ground slope according to which operating pressure heads along the
401 entire downhill lateral are in the desired range, assuming its maximum admissible value at the
402 manifold connection and at the end of the lateral and its minimum admissible in a generic
403 section of the lateral. This threshold ground slope tends to increase at increasing h_n or at
404 decreasing S .

405 The validation of the proposed approach has been then assessed in terms of its ability to
406 predict the variations of pressure heads along the lateral and consequently to estimate the
407 distribution of emitter flow rates, according to the actual flow rate-pressure head relationship.
408 In particular, application of the iterative forward step-by-step (SBS) procedure, evidenced that
409 the value of pressure head corresponding to the generic emitter tends to rise at increasing
410 values of the exponent x , of the flow rate-pressure head relationship. However, the maximum
411 differences of operating pressure heads along the entire lateral, for $x=0.5$ and $x=1.0$ resulted
412 respectively equal to -1.12 % and -1.74 % for the first examined case, and to -1.47 % and -
413 2.24 % for the second.

414 According to the recognized pressure head, the maximum error associated to the discharged
415 flow rates in the first case resulted always lower than -0.56 % ($x = 0.5$) and -1.74 % ($x = 1.0$),
416 whereas in the second case, lower than -0.74 % ($x = 0.5$) and -2.24 % ($x = 1.0$) and hence in
417 both the examined examples insignificant for practical applications.

418

419 **Acknowledgements**

420

421 Research was co-financed by Ministero dell'Istruzione, dell'Università e della Ricerca
422 (MIUR) and FFR 2012-2013 granted by Università degli Studi di Palermo. The contribution
423 to the manuscript has to be shared between authors as following: Theory and applications of
424 the proposed procedure were carried out by Giorgio Baiamonte. All the authors analyzed
425 results and wrote the text. The Authors wish to thank the anonymous reviewers for the helpful
426 comments and suggestions during the revision stage.

427

428 **List of symbols**

429

430 D [m] internal pipe diameter

431 f [-] friction factor

432 g [m^2/s] acceleration of gravity

433 h_i [m] pressure head of the generic emitter i

434 $h_i^{(u)}$ [m] pressure head of the i -th emitter in the uphill lateral

435 $h_i^{(d)}$ [m] pressure head of the i -th emitter in the downhill lateral

436 $h_{min}^{(u)}$ [m] minimum pressure head in the uphill lateral

437 $h_{max}^{(u)}$ [m] maximum pressure head at the manifold connection

438 $h_{min}^{(d)}$ [m] minimum pressure head in the downhill lateral

439 $h_{max}^{(d)}$ [m] maximum pressure head at the downhill end of the lateral

440 h_n [m] nominal emitter's pressure head

441 $H(.,.)$ generalised harmonic number

442 i [-] generic emitter of the lateral counted from the manifold connection

443 i_{min} [-] number of emitters in downhill lateral, from the manifold connection to the section
444 with minimum pressure head

445 J [-] friction losses per unit pipe length

446 K (-) parameter

447 L [m] length of the lateral

448 L_{opt} [m] optimal (maximum) length of the lateral
 449 n [-] total number of emitters in the entire lateral
 450 n_u [-] number of emitters in the uphill lateral
 451 n_d [-] number of emitters in the downhill lateral
 452 $n_{d,opt}^{th}$ [-] optimal number of emitters in the downhill lateral corresponding to S_0^{th} [%]
 453 n_{opt}^{th} [-] optimal number of emitters in the entire lateral corresponding to S_0^{th} [%]
 454 n_{opt} [-] optimal number of emitters in the lateral
 455 n_x [-] generic emitter of the lateral counted from the uphill end of the lateral
 456 q_n [$m^3 s^{-1}$] nominal emitter discharge
 457 R [-] Reynolds number
 458 S [m] emitter spacing
 459 S_0 [%] slope of the lateral
 460 S_0^{th} [%] threshold ground slope for which operating pressure head at the end of the downhill
 461 lateral is equal to $1.1 h_n$
 462 V [m/s] mean flow velocity
 463 x [-] exponent of the flow rate-pressure head relationship
 464 $\Delta h_f^{(d)}$ [m] total friction losses in the downhill lateral
 465 $\Delta h_f^{(u)}$ [m] total friction losses in the uphill lateral
 466 γ_n Stieltjes constants
 467 ν [$m^2 s^{-1}$] kinematic water viscosity
 468 ζ Riemann Zeta function
 469

470 **References**

471

472 Agnese, C., Baiamonte, G. and Cammalleri, C. (2014). “Modelling the occurrence of rainy
473 days in a typical Mediterranean.” *Adv. Water Resources* 64, 62-76,
474 <http://dx.doi.org/10.1016/j.advwatres.2013.12.005>.

475 Al-Amoud, A. I. (1995). “Significance of energy losses due to emitter connections in trickle
476 irrigation lines.” *J. Agric. Eng. Res.*, 60(1), 1–5.

477 Al-Samarmad, O.T. (2002). “Optimum Dimension of a trickle irrigation subunit by using
478 local prices”. *M. Sc. Thesis*, Dept. of Irrig. and Drain. Eng., Coll. of Eng., University of
479 Baghdad, Iraq.

480 Bagarello, V., Ferro, V., Provenzano, G., and Pumo, D. (1997). “Evaluating pressure losses in
481 drip-irrigation lines”. *J. Irrig. Drain. Eng.*, 123(1), 1–7.

482 Genius, M., Koundouriy, P., Naugesz, C., and Tzouvelekas V. (2012). “Information
483 transmission in irrigation technology adoption and diffusion: Social learning, extension
484 services and spatial effects”. *Working Paper 1211*. Dept. of Economics, University of Crete.

485 Gill, P.E., Murray, W., and Wright, M.H. (1989). “Practical optimization”. *Academic Press,*
486 *Inc.*, San Diego, Calif., 90-91.

487 Jiang, S., and Kang, Y. (2010). “Simple method for the design of microirrigation paired
488 laterals”. *J. Irrig. Drain. Eng.*, 136(4), 271-275.

489 Juana, L., Rodriguez-Sinobas, L., and Losada, A. (2002). “Determining minor head losses in
490 drip irrigation laterals. I: Methodology”. *J. Irrig. Drain. Eng.*, 128(6), 376–384.

491 Kang, Y., and Nishiyama, S. (1996). “Analysis and design of microirrigation laterals”. *J.*
492 *Irrig. Drain. Eng.*, 122(2), 75-82.

493 Kang, Y., Nishiyama, S., and Chen, H. (1996). “Design of microirrigation laterals on
494 nonuniform slopes”. *Irrig. Sci.* 17:3-14.

495 Karmeli, D., and Keller, J. (1975). “Trickle irrigation design”. *Rain Bird Sprinkler*
496 *Manufacturing Corporation, Glendora, Calif.*

497 J. Keller, and Bliesner, R.D. (2001). *Sprinkle and Trickle Irrigation*. The Blackburn Press,
498 New York, pp: 652. ISBN-13: 978-1930665194

499 Provenzano, G. (2005). Discussion of “Analytical Equation for variation of discharge in drip
500 irrigation laterals” by V. Ravikumar, C.R. Ranganathan, and S. Santhana Bosu. *J. Irrig.*
501 *Drain. Eng.*, 129(4), 295-298.

502 Provenzano, G., Pumo D., and Di Dio, P. (2005). “Simplified procedure to evaluate head
503 losses in drip irrigation laterals”. *J. Irrig. Drain. Eng.*, 131(6), 525-532.

504 Provenzano, G., Di Dio, P., Palau Salvador, G. (2007). “New computation fluid dynamic
505 procedure to estimate friction and local losses in coextruded drip laterals”. *J. Irrig. Drain.
506 Eng.*, 133(6), 520-527.

507 Provenzano, G., Di Dio, P., Leone, R. (2014). “Assessing a local losses evaluation procedure
508 for low-pressure, lay-flat drip laterals”. Accepted on *J. Irrig. Drain. Eng.*

509 Wu, I.P. (1975). “Design of drip irrigation main lines”. *J. Irrig. and Drain. Div.*, 101(IR4),
510 265-278.

511 Wu, I.P., and Gitlin, H.M. (1975). “Energy gradient line for drip irrigation laterals”. *J. Irrig.
512 and Drain. Div.*, 101(IR4), 321-326.

513 Wu, I.P., Gitlin, H.M., Solomon, K.H., and Saruwatari, C.A. (1986). “Design principles:
514 Trickle irrigation for crop production”. In *F.S. Nakayama and D.A. Bucks, eds., Elsevier
515 Science*, Phoenix, 53-92.

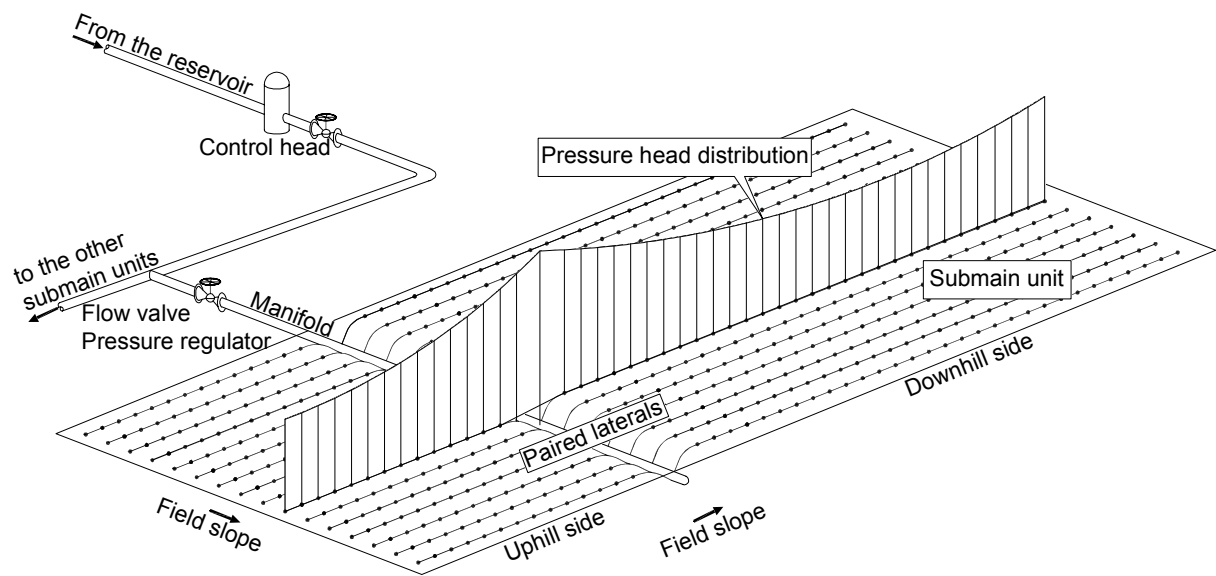


Fig. 1 – Schematic layout of a submain unit with paired laterals. The pressure head distribution line for a generic lateral is also indicated.

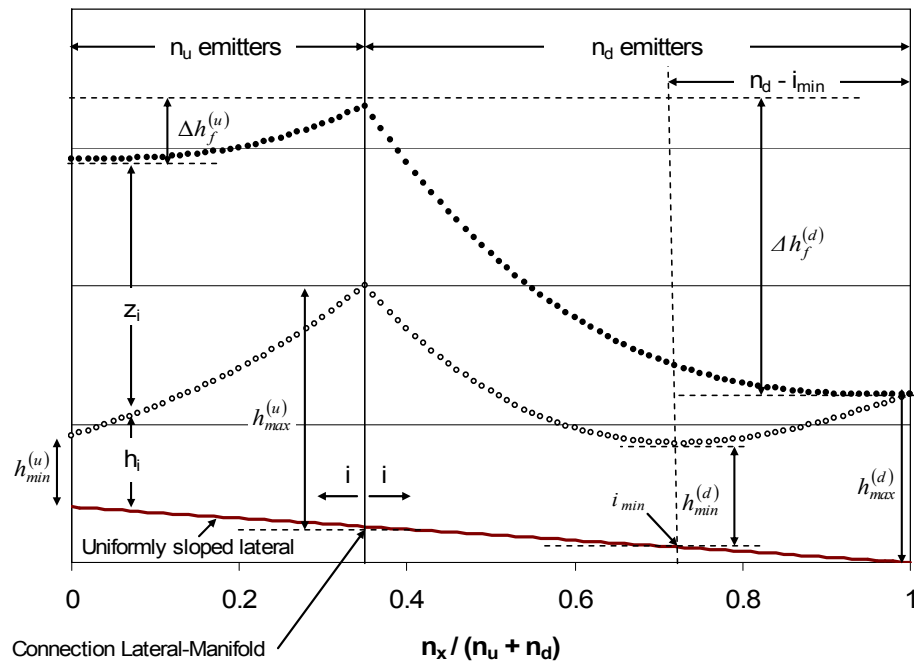


Fig. 2 – Scheme of a microirrigation paired lateral laid on a uniformly sloped field. White and black dots indicate the pressure head distribution and the hydraulic grade line, respectively.

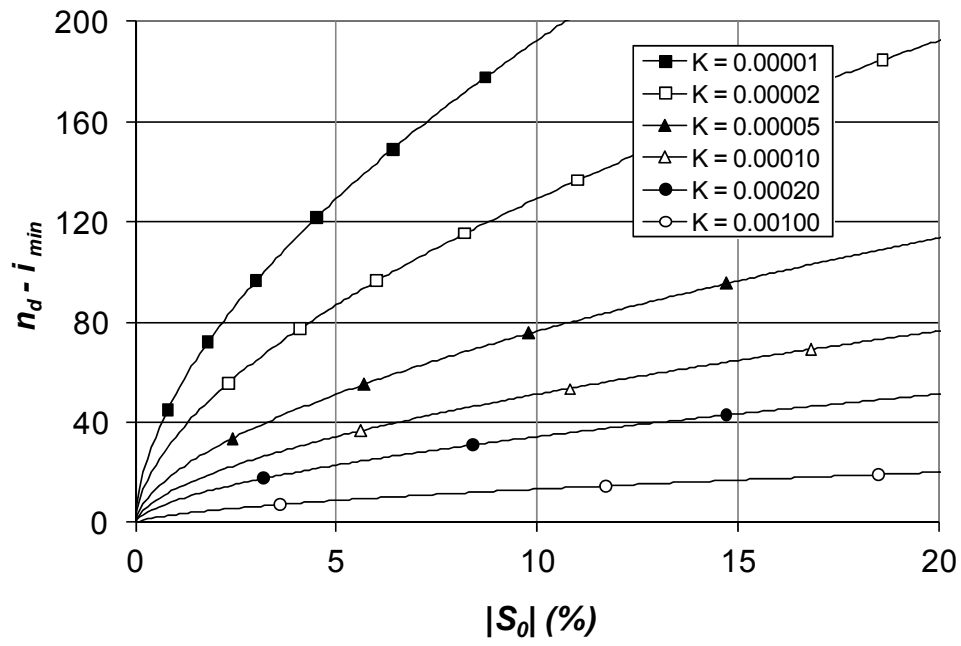


Fig. 3 – Relative position of the emitter characterized by the minimum pressure head along the lateral as a function of $|S_0|$, for different values of the constant K .

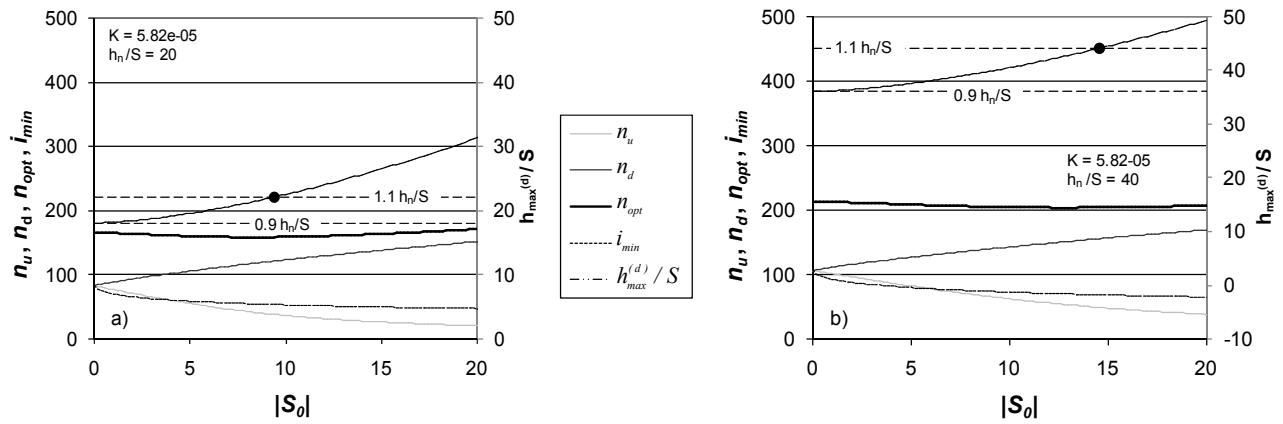


Figure 4 – Number of emitters in the uphill lateral, n_u , evaluated with eq. 9, pairs (n_d, i_{min}) obtained by eqs. (13) and (14), and sum $n_{opt} = n_d + n_u$, as a function of the lateral slope $|S_0|$, for $K = 5.82 \times 10^{-5}$, $h_n/S = 20$ (a) and $h_n/S = 40$ (b). In the secondary vertical axes, the dimensionless nominal pressure head at the end of the downhill lateral, hn_d/S , as well as the minimum and the maximum admissible, $0.9 h_n/S$ and $1.1 h_n/S$, are also indicated. Black dots indicate the slope threshold value, $|S_0^{th}|$.

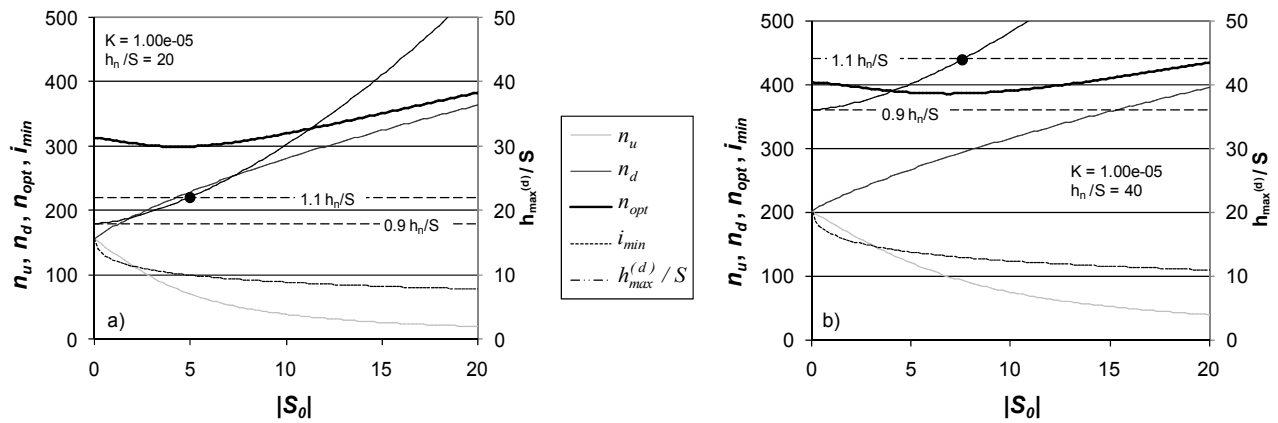


Figure 5 – Number of emitters in the uphill lateral, n_u , evaluated with eq. 9, pairs (n_d, i_{min}) obtained by eqs. (13) and (14), and sum $n_{opt} = n_d + n_u$, as a function of the lateral slope $|S_0|$, for $K = 1.00e-05$, $h_n/S = 20$ (a) and $h_n/S = 40$ (b). In the secondary vertical axes, the dimensionless nominal pressure head at the end of the downhill lateral, h_{nd}/S , as well as the minimum and the maximum admissible, $0.9 h_n/S$ and $1.1 h_n/S$, respectively. Black dots indicate the slope threshold value, $|S_0^{th}|$.

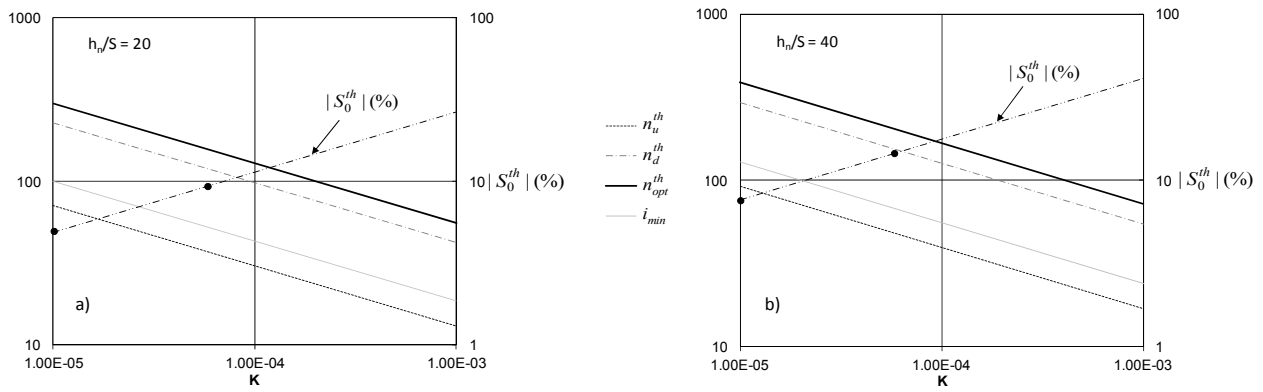


Figure 6 – Number of the threshold emitters in the uphill lateral, n_u^{th} , and in the downhill lateral n_d^{th} , corresponding location of the emitter with the minimum pressure head, i_{min} , and optimal number of emitters in the entire sloped lateral $n_{opt}^{th} = n_u^{th} + n_d^{th}$, as a function of K , for $h_n/S = 20$ (a) and for $h_n/S = 40$ (b). In the secondary vertical axes, the slope threshold $|S_0^{th}|$ is also represented. Black dots indicate the slope thresholds corresponding to $h_n/S = 20$ (Figs. 4a and 5a), and to $h_n/S = 40$ (Figs. 4b and 5b).

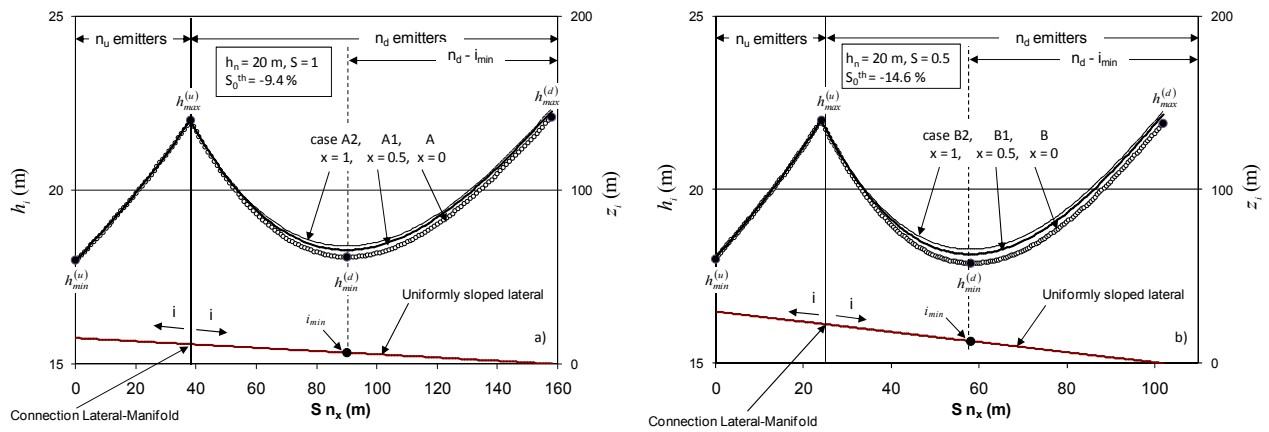


Figure 7 – Distributions of pressure heads along the lateral for case A (a) and B (b), under the hypothesis of constant emitter flow rates ($x = 0$) or assuming the other two flow rate-pressure head relationships obtained for $x = 0.5$ and $x = 1.0$.

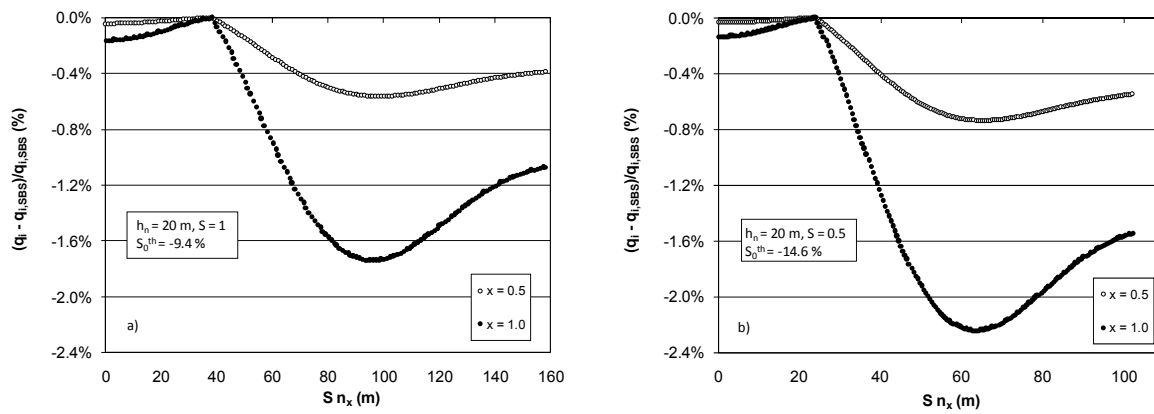


Figure 8 – Errors on flow rates, as a function of the lateral length, calculated by considering the pressure head distribution obtained with the proposed approach ($x = 0$) and the corresponding actual values determined by using the SBS procedure with exponents of the flow rate-pressure head relationship equal to 0.5 and = 1.0.

FIGURE CAPTIONS

Fig. 1 – Schematic layout of a submain unit with paired laterals. The pressure head distribution line for a generic lateral is also indicated.

Fig. 2 – Scheme of a microirrigation paired lateral laid on a uniformly sloped field. White and black dots indicate the pressure head distribution and the hydraulic grade line, respectively.

Fig. 3 – Relative position of the emitter characterized by the minimum pressure head along the lateral as a function of $|S_0|$, for different values of the constant K .

Figure 4 – Number of emitters in the uphill lateral, n_u , evaluated with eq. 9, pairs (n_d, i_{min}) obtained by eqs. (13) and (14), and sum $n_{opt} = n_d + n_u$, as a function of the lateral slope $|S_0|$, for $K = 5.82e-05$, $h_n/S = 20$ (a) and $h_n/S = 40$ (b). In the secondary vertical axes, the dimensionless nominal pressure head at the end of the downhill lateral, hn_d/S , as well as the minimum and the maximum admissible, $0.9 h_n/S$ and $1.1 h_n/S$, are also indicated. Black dots indicate the slope threshold value, $|S_0^{th}|$.

Figure 5 – Number of emitters in the uphill lateral, n_u , evaluated with eq. 9, pairs (n_d, i_{min}) obtained by eqs. (13) and (14), and sum $n_{opt} = n_d + n_u$, as a function of the lateral slope $|S_0|$, for $K = 1.00e-05$, $h_n/S = 20$ (a) and $h_n/S = 40$ (b). In the secondary vertical axes, the dimensionless nominal pressure head at the end of the downhill lateral, hn_d/S , as well as the minimum and the maximum admissible, $0.9 h_n/S$ and $1.1 h_n/S$, respectively. Black dots indicate the slope threshold value, $|S_0^{th}|$.

Figure 6 – Number of the threshold emitters in the uphill lateral, n_u^{th} , and in the downhill lateral n_d^{th} , corresponding location of the emitter with the minimum pressure head, i_{min} , and optimal number of emitters in the entire sloped lateral $n_{opt}^{th} = n_u^{th} + n_d^{th}$, as a function of K , for $h_n/S = 20$ (a) and for $h_n/S = 40$ (b). In the secondary vertical axes, the slope threshold $|S_0^{th}|$ is also represented. Black dots indicate the slope thresholds corresponding to $h_n/S = 20$ (Figs. 4a and 5a), and to $h_n/S = 40$ (Figs. 4b and 5b).

Figure 7 – Distributions of pressure heads along the lateral for case A (a) and B (b), under the hypothesis of constant emitter flow rates ($x = 0$) or assuming the other two flow rate-pressure head relationships obtained for $x = 0.5$ and $x = 1.0$.

Figure 8 – Errors on flow rates, as a function of the lateral length, calculated by considering the pressure head distribution obtained with the proposed approach ($x = 0$) and the corresponding actual values determined by using the SBS procedure with exponents of the flow rate-pressure head relationship equal to 0.5 and = 1.0.